INFLUENCE OF THERMOSENSITIVITY OF MATERIALS ON THE TEMPERATURE OF A PAD/DISC SYSTEM

Piotr GRZEŚ[*]

[*]PhD Student, Faculty of Mechanical Engineering, Bialystok University of Technology,
Wiejska 45 C, 15 351 Bialystok

p.grzes@doktoranci.pb.edu.pl

Abstract: A heat generation problem due to friction in a pad/disc brake system is studied. A linear problem is confronted and compared with a non-linear in which thermophysical properties of materials are temperature-dependent. To examine temperature of the pad and the disc during a single and a twofold braking process, axisymmetric FE contact model was used. The obtained results revel insignificant temperature differences at specified axial and radial positions of the components of the friction pair. It was remarked that the level of discrepancies between the constant and the thermosensitive materials correspond with the coefficient of thermal effusivity.

1. INTRODUCTION

Inherent heat generation during slipping of contacting bodies leads to an increase in temperature on the friction surfaces. Over the decades analytical and numerical models have been developed to improve the accuracy and repeatability of the obtained by their means solutions in application to various types of brake systems (Scieszka, 1998). Despite the fact that the analytical methods provide exact solutions on which numerical calculations are based, advantage of the latter is noticeable in application to complex objects with finite dimensions and non-linear problems (Yi et al., 2002; Scieszka and Zolnierz, 2007; Aderghal et al., 2011).

Parameters of braking operation such as a contact pressure, a sliding velocity, a coefficient of friction, cooling conditions are frequently brought to constant values aiming to distinguish markedly an impact of chosen factors. Adamowicz and Grzes (2011a) developed and compared axisymmetric two-dimensional and fully three-dimensional models of a disc rotor during a single emergency braking process. Braking operation with the constant as well as linearly decreasing velocity of a vehicle was studied to evaluate its influence on the temperature distributions of a disc. On the basis of that FE modelling technique the effects of cooling conditions during a period of braking with constantly rotating disc from adiabatic conditions to the firmly forced convection (100 W/(m^{2}K)) were studied in ref. (Adamowicz and Grzes, 2011b).

If the system operates markedly above a certain temperature, the friction materials can vary their thermophysical properties affecting the conditions of contact and in consequence a non-linear problem is apparent. Nonetheless only few numerical calculations deal with the temperature-dependent thermophysical properties of materials in application to brake systems (Lee and Barber, 1994; Thuresson, 2004; Sergienko 2009).

This study aims to examine an effect of thermosensitive materials on the thermal behaviour of a pad/disc tribo-system. The corresponding temperatures are confronted with the values of the model which operate within theirs constant equivalents. FE 2D contact model was used based on the author's previous study (Grzes, 2010). The properties of materials were adopted and approximated by using methodology with the three constants (Chichinadze et al., 1979).

2. STATEMENT OF THE PROBLEM

The frictional heat generation in a disc brake in actual is accompanied by its dissipation through the three known modes of heat transfer. The conduction absorbs energy from the pad/disc interface by the neighbouring parts of the brake assembly and hub. The convection exchanges heat from the exposed surfaces with the surrounding environment according to Newton's law of cooling. Typically disc brakes have vanes whose presence allows to enlarge the area of convective heat transfer, however evident advantages of such type of a rotor emerges during a long-lasting processes after disconnection of the sliding bodies or during a multiple brake application (Adamowicz and Grzes, 2011b). The remaining phenomenon that intensifies cooling of the brake is the thermal radiation. However its share in total heat dissipation is frequently ignored due to attained maximal temperatures and the duration of the analyzed process. Thereby in this study solely conduction and convection are taken into account.

The mechanisms of the pad operation through the caliper during brake application vary. However it is stated that the amount of heat generated during friction for certain dimensions of a rubbing path and assumed constant uniform contact pressure remains equal. The converted mechanical energy is assumed to be entirely used for the heat, whose magnitude expresses the capacity of friction power and in application to the rotating system has the following form:

$$q(t) = fr\omega(t)p_0 \qquad (1)$$

where: f – friction coefficient, $\omega(t)$ – angular velocity, t – time, r – radial coordinate, p_0 – contact pressure.

The separation of heat between contacting bodies may be proceeded in two ways. One of frequently used approaches is a calculation of temperature fields by means of two individual bodies/models (a stator and a rotor) introducing a heat partition ratio (Grzes, 2009; 2011) and other is a use of contact model which is employed in this study (Bialecki and Wawrzonek, 2008). It is established that the separation of heat between the pad and the disc varies during the process satisfying two conditions of the perfect thermal contact on the corresponding friction surfaces:

$$T(r_i, 0^+, t) = T(r_j, 0^-, t), \ r_p \leq r \leq R_p, \ 0 \leq t \leq t_s, \qquad (2)$$

$$K_d(T)\frac{\partial T}{\partial z}\bigg|_{z=0^-} - K_p(T)\frac{\partial T}{\partial z}\bigg|_{z=0^+} = q(r,t) \equiv fr\omega(t)p_0, \qquad (3)$$

$$r_p \leq r \leq R_p, \ 0 \leq t \leq t_s,$$

where: $+(-)$ denotes value obtained at the approach toward plane $z = 0$ from the $+(-)$ side of the axis OZ, T – temperature, i, j – the pad and the disc corresponding radial locations on the contact surface, d, p – the disc and the pad, respectively, r, R – internal and external radius, respectively.
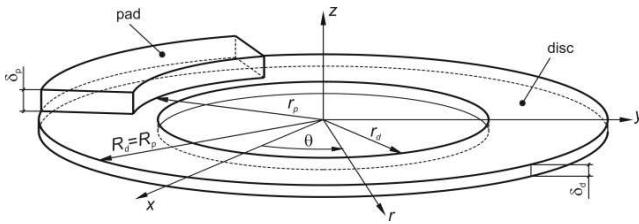
Fig. 1. Schematic diagram of half of a pad/disc brake system

Angular velocity of the rotor decreases linearly from the initial value ω_0 to full stop according to formula:

$$\omega(t) = \omega_0\left(1 - \frac{t}{t_s}\right), \ 0 \leq t \leq t_s, \qquad (4)$$

where: t_s – braking time.

3. MATHEMATICAL FORMULATION

The governing equation for the heat conduction analysis was the parabolic heat conduction equation given in the cylindrical coordinate system (r, z):

$$\frac{\partial}{\partial r}\left(K_{d,p}(T)\frac{\partial T}{\partial r}\right) + \frac{K_{d,p}(T)}{r}\frac{\partial T}{\partial r} + \qquad (5)$$

$$+ \frac{\partial}{\partial z}\left(K_{d,p}(T)\frac{\partial T}{\partial z}\right) = \rho_{d,p}\, c_{d,p}(T)\frac{\partial T}{\partial t}$$

where: z – axial coordinate, $K(T)$ – thermal conductivity, ρ – density, $c(T)$ – specific heat.

In order to determine the transient temperature distributions in the brake components during frictional sliding process both analytical and numerical techniques were employed. Lack of the circumferential component in the above governing equation stems from the assumption that neither non-axisymmetric thermal load acting as the intensity of heat flux directed into the disc and the pad nor the resulting heat flow in the circumference, doesn't affect significantly an average temperature generated at the pad/disc interface above certain relative sliding velocity (Peclet number Pe).

The boundary and initial conditions (Fig. 2) are the following:
– on the free surfaces of the pad:

$$K_p(T)\frac{\partial T}{\partial r}\bigg|_{r=r_p} = h[T(r_p, z, t) - T_a], \ 0 \leq z \leq \delta_p, \ 0 \leq t \leq t_s, \qquad (6)$$

$$K_p(T)\frac{\partial T}{\partial r}\bigg|_{r=R_p} = h[T_a - T(R_p, z, t)], \ 0 \leq z \leq \delta_p, \ 0 \leq t \leq t_s, \qquad (7)$$

$$\frac{\partial T}{\partial z}\bigg|_{z=\delta_p} = 0, \ r_p \leq r \leq R_p, \ 0 \leq t \leq t_s, \qquad (8)$$

where: h – heat transfer coefficient, T_a – ambient temperature, T_0 – initial temperature, δ – thickness.
– and the free surfaces of the disc:

$$K_d(T)\frac{\partial T}{\partial z}\bigg|_{z=0} = h[T_a - T(r, 0, t)], \ r_d \leq r \leq r_p, \ 0 \leq t \leq t_s, \qquad (9)$$

$$\frac{\partial T}{\partial r}\bigg|_{r=r_d} = 0, \ -\delta_d \leq z \leq 0, \ 0 \leq t \leq t_s \qquad (10)$$

$$K_d(T)\frac{\partial T}{\partial r}\bigg|_{r=R_d} = h[T_a - T(R_d, z, t)], \ -\delta_d \leq z \leq 0, \ 0 \leq t \leq t_s \qquad (11)$$

$$\frac{\partial T}{\partial z}\bigg|_{z=-\delta_d} = 0, \ r_d \leq r \leq R_d, \ 0 \leq t \leq t_s \qquad (12)$$

At the initial time moment $t = 0$ the pad and disc are heated to the same constant temperature:

$$T(r, z, 0) = T_0, \ r_p \leq r \leq R_p, \ 0 \leq z \leq \delta_p, \qquad (13)$$

$$T(r, z, 0) = T_0, r_d \leq r \leq R_d, \ -\delta_d \leq z \leq 0. \qquad (14)$$

where: T_0 – initial temperature.

4. NUMERICAL FORMULATION

The object of this section is to develop approximate time-stepping procedures for axisymmetric transient governing equations.

Using Galerkin's method the following matrix form of the Eq. (5) is formulated (Lewis et al., 2004)

$$[C(T)]\left\{\frac{dT}{dt}\right\} + [K(T)][T] = \{R\} \qquad (15)$$

where: $[C(T)]$ is the heat capacity matrix, $[K(T)]$ is the heat conductivity matrix, and $\{R\}$ is the thermal force vector.

In order to solve the ordinary differential equation (15)

the direct integration method was used. Based on the assumption that temperature $\{T\}_t$ and $\{T\}_{t+\Delta t}$ at time t and $t+\Delta t$ respectively, the following relation is specified

$$\{T\}_{t+\Delta t} = \{T\}_t + \left[(1-\beta)\left\{\frac{dT}{dt}\right\}_t + \beta\left\{\frac{dT}{dt}\right\}_{t+\Delta t}\right]\Delta t \qquad (16)$$

Substituting Eq. (16) to Eq. (15) we obtain the following implicit algebraic equation

$$
\begin{aligned}
&([C(T)] + \beta\Delta t[K(T)])\{T\}_{t+\Delta t} = \\
&([C(T)] - (1-\beta)[K(T)]\Delta t)\{T\}_t + \\
&+ (1-\beta)\Delta t\{R\}_t + \beta\Delta t\{R\}_{t+\Delta t}
\end{aligned}
\qquad (17)
$$

where: β is the factor which ranges from 0,5 to 1 and is given to determine an integration accuracy and stable scheme.
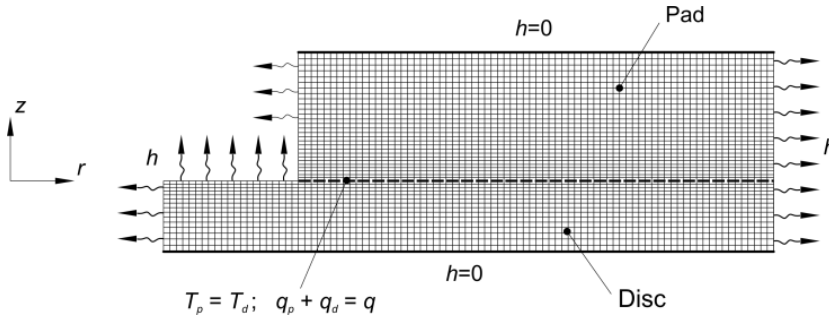
Fig. 2. Finite element mesh of a disc brake

FE axisymmetric 2D model is shown in Fig. 2. Four node quad type elements were used. Total number of elements of the brake model equals 3497, in which 1425 elements and 1536 nodes come to the disc, and 2072 elements and 2175 nodes come to the pad.

The heating of the friction surfaces was accomplished by means of the total intensity of heat flux directed into the pad. Furthermore by using 75 'multi point constraints' MPC at subsequent pairs of nodes of the friction surfaces of the pad and the disc separation according to boundary conditions Eqns. (2,3) during simulated slipping contact took place (constraint of the temperatures). Other surfaces (edges in the FE model) were either cooled or insulated satisfying Eqns. (6-14).

5. RESULTS AND DISCUSSION

In the study thermal finite element analysis of heat generation due to friction in a pad/disc brake system was carried out. The temperature evolutions at specified axial and radial positions obtained incorporating the temperature-independent thermophysical properties of materials are calculated and compared with the thermosensitive materials.

5.1. Operation parameters and dimensions of the pad/disc system

Operation parameters and dimensions of the brake are listed in Tab. 1. The single braking process proceeds during 3,96 s from the initial velocity of 100 km/h ($\omega_0 = 88,464$ s^{-1}) to standstill with constant retardation (Talati and Jalalifar 2009). In order to develop twofold braking process the boundaries conditions after the disengagement of the braking components obviously had to be diverse. The total time of the twofold braking process equalled $t_s = 40$ s. The brak-

ing schema was as follows, after the moment of full stop a vehicle increased velocity with constant acceleration to the velocity of 100 km/h during 16.04 s. Then the cycle was repeated attaining 40 s of the total twofold braking operation. Despite the fact of change of the velocity the heat transfer coefficient remained constant (Tab. 2) which was due to the fact of its insignificant impact on the resulting temperature distributions.

Tab. 1. Operation parameters and dimensions of the disc and the pad (Talati and Jalalifar, 2009)

item	disc	pad
inner radius, r [m]	0,066	0,0765
outer radius, R [m]	0,1135	0,1135
thickness, δ [m]	0,0055	0,01
initial angular velocity of the rotor, ω_0 [s^{-1}]	88,464	
single/twofold braking time, t_s [s]	3,96/40	
heat transfer coefficient, h [W/(m^{2}K)]	60	
contact pressure, p_0 [Pa]	1.47×10^6	
coefficient of friction, f	0,5	
initial temperature, T_0 [°C]	20	
ambient temperature, T_a [°C]	20	

5.2. Thermophysical properties of materials

Behaviour of the material properties under the influence of temperature were derived from the measurements carried out in ref. (Chichinadze et al., 1979). To obtain mathematical formulas of variations of the essential in thermal analysis thermophysical properties of materials, the methodology proposed in that paper was used as well. Two of the three available crucial for the calculations properties were chosen having in mind possibly the smoothest temperature dependence. Thus despite the fact that the employed FE based

programme required specific heat c and thermal conductivity K, only the latter satisfied the criterions. The second parameter was the thermal diffusivity k whose value allowed to calculate required specific heat.

Below approximate formulas for the thermal conductivity and the thermal diffusivity of four different materials used in numerical computations are listed:

− for the pad materials:
− FMK-845

$$K_p(T) = 9.806\left(1.171 + \frac{1.315}{1 + 7.32 \cdot 10^{-7} \cdot T^2}\right) \quad (18)$$

$$k_p(T) = 10^{-6}\left(-0.823 + \frac{10.778}{1 + 1.487 \cdot 10^{-6} \cdot T^2}\right) \quad (19)$$

− FMK-11

$$K_p(T) = 9.806\left(4.017 + \frac{-2.282}{1 + 5.298 \cdot 10^{-6} \cdot (T - 900)^2}\right) \quad (20)$$

$$k_p(T) = 10^{-6}\left(-1.146 + \frac{17.207}{1 + 2.122 \cdot 10^{-6} \cdot (T + 100)^2}\right) \quad (21)$$

− and for the disc:
− steel EI-696

$$K_d(T) = 0.014T + 15.727 \quad (22)$$

$$k_d(T) = -1.444 \cdot 10^{-9} T + 5.502 \cdot 10^{-6} \quad (23)$$

− cast iron ChNMKh

$$K_d(T) = -0.028T + 52.727 \quad (24)$$

$$k_d(T) = 10^{-6}\left(5.557 + \frac{15.226}{1 + 8.018 \cdot 10^{-6}(T + 400)^2}\right) \quad (25)$$

The presented formulas for the thermal conductivity and the thermal diffusivity have their equivalent at approximately 20 °C which are shown in Tab. 2. As can be seen the major differences between temperature-independent thermophysical properties of materials of the disc (steel EI-696, cast iron ChNMKh) is encountered for the thermal conductivity K. Less distinct are the constant properties of the pad FMK-845, FMK-11). However for the thermo-sensitive materials together with the temperature their values vary in a different way (Figs. 3, 4) giving possibility to examine such a behaviour on the temperatures of the pad and the disc.

Tab. 2. Thermophysical properties of materials independent of temperature (Chichinadze et al., 1979)

material	K [W/(mK)]	k [m²/s]	ρ [kg/m³]
EI-696	16,3	4,92×10⁻⁶	7850
ChNMKh	51	1,44×10⁻⁵	7100
FMK-845	24,5	1,04×10⁻⁵	6000
FMK-11	34,3	1,46×10⁻⁵	4700

Using formulas 18-25 particular properties were calculated and set tabularly into the commercial finite element based programme (MSC.SOFTWARE). The step of the

temperature was equal 0.1 °C giving consequently 8001 lines. Moreover it was established that the closest value of the given property from the table was selected during the calculations.
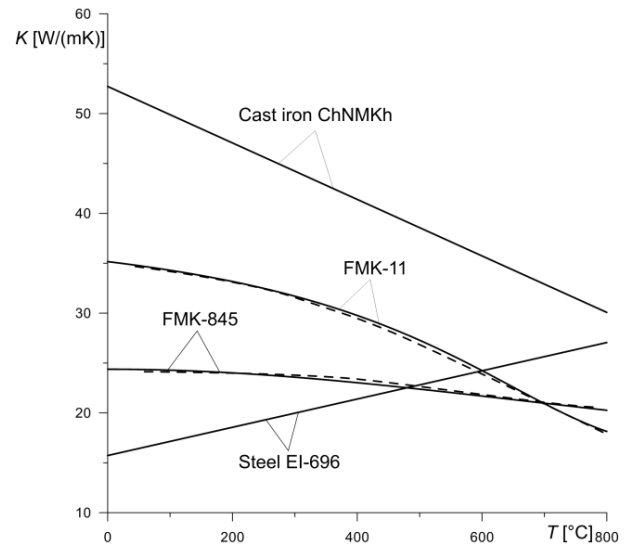
Fig. 3. Thermal conductivities of a disc and a pad versus temperature obtained from the measurements (solid curves) and their approximations (dashed curves) (Chichinadze et al., 1979)
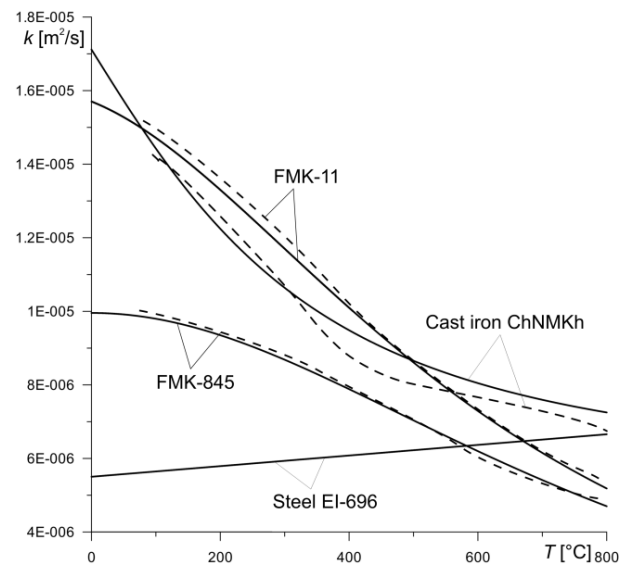
Fig. 4. Thermal diffusivities of a disc and a pad versus temperature obtained from the measurements (solid curves) and their approximations (dashed curves) (Chichinadze et al., 1979)

As a result of the carried out computations evolutions of temperature at the pad/disc interface (equal temperature on the pad and the disc friction surfaces at specified radial positions) are shown. In Fig. 5 the temperature evolutions are depicted for two braking couples, for the disc made of cast iron ChNMKh and two different pad materials FMK-845 (Fig. 5a) and FMK-11 (Fig. 5b).

As can be seen the temperatures on the friction surfaces are smooth not revealing any periods of interchangeable heating and cooling which stems from the main as-

sumptions of this study of axisymmetric heat flux distribution and perfect contact between the pad and the disc. Comparison of two- and three-dimensional axisymmetric models was shown is ref. (Adamowicz and Grzes, 2011a). Evolutions of temperature of the thermosensitive materials and their temperature-independent equivalents are marked with dashed and solid lines, respectively. All further plots will have the same denotation. The obtained results make evident that during the considered single braking operation, variations of the thermal conductivity and thermal diffusivity (Fig. 3, 4) do not allow to change firmly the contact temperatures of the disc brake at any of the radial positions. However the highest temperature difference between these two friction couplings is observable at the biggest distance from the axis of rotation z.

In Fig. 6 temperatures of the disc at different axial positions and constant radius $r = 0,095$ m are related to the braking time. Previous material compositions (Fig. 5) are confronted again. The distances between illustrated z positions are not constant to enable clear visualisation of the results. Since the disc is located under the radial coordinate axial values are plotted with minus. Obviously it can be seen that the temperatures are lower with the increase of z distance. Until half of the braking time t_s temperatures at each location in axial direction almost coincide (regarding thermosensitive and temperature-independent materials). After that time temperatures of the model with thermosensitive materials are slightly lower, however, revealing the same behaviour as materials with constant properties.
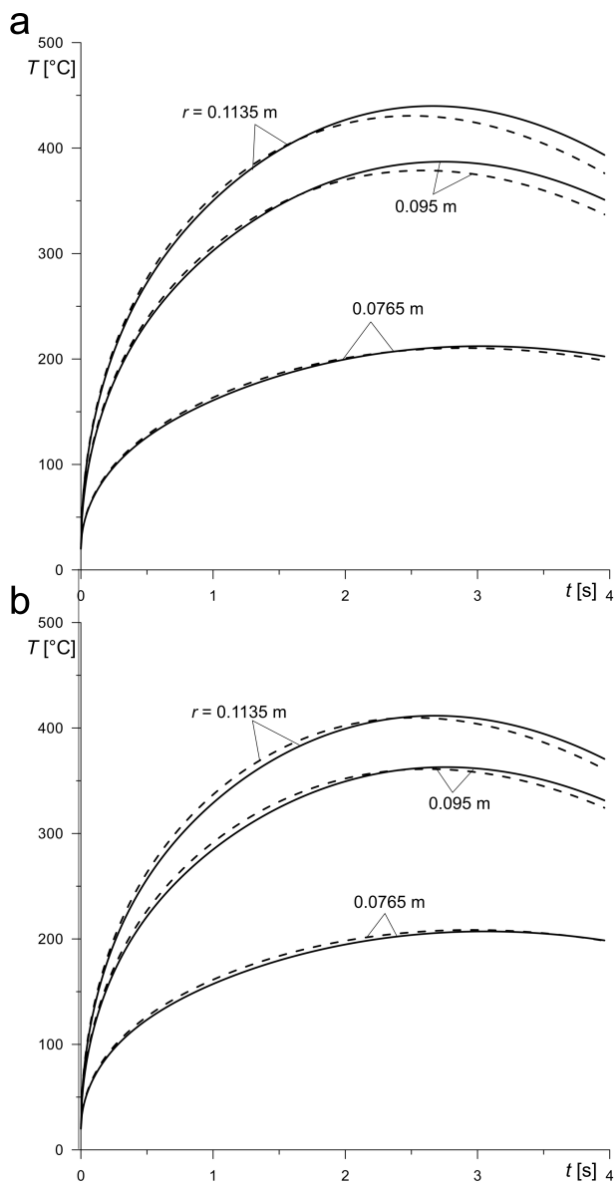
Fig. 5. Evolutions of temperature at the pad/disc interface
for different radial positions, solid curves indicate
temperature-independent thermophysical properties
whereas dashed curves thermosensitive materials:
a) disc (cast iron ChNMKh)/pad (FMK-845)
b) disc (cast iron ChNMKh)/pad (FMK-11)
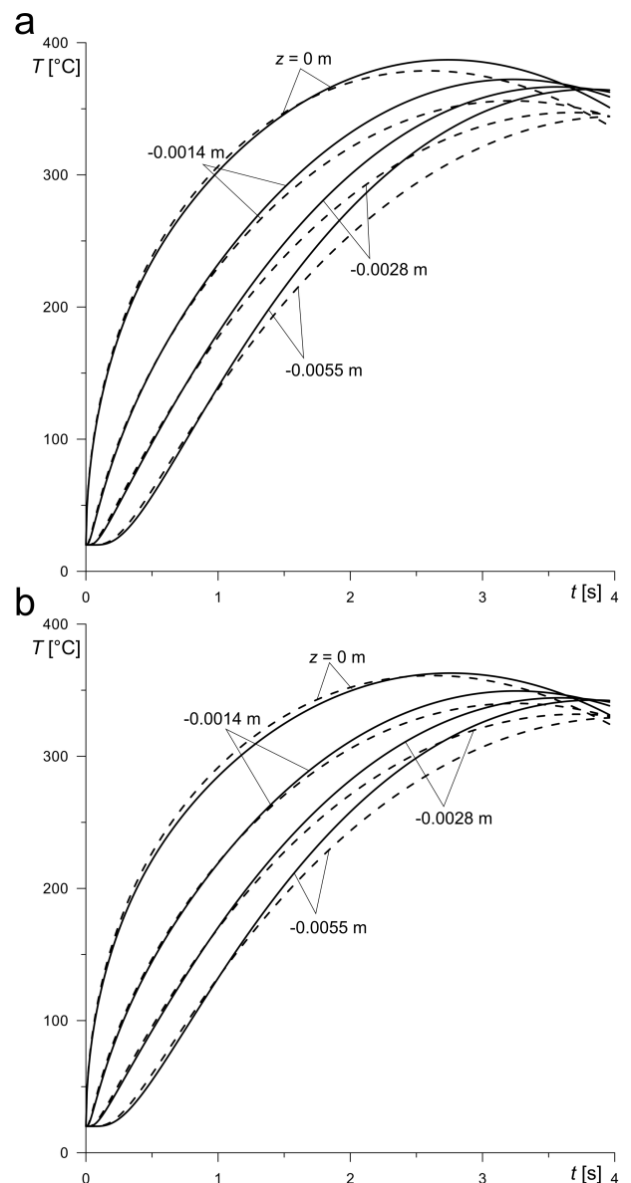
Fig. 6. Evolutions of temperature at different radial axial
positions of a disc (r = 0.095 m), solid curves indicate
temperature-independent thermophysical properties
whereas dashed curves thermosensitive materials:
a) disc (cast iron ChNMKh)/pad (FMK-845)
b) disc (cast iron ChNMKh)/pad (FMK-11)

Temperature evolutions at the pad/disc interface for the disc made of steel EI-696 and two different pad materials (the same as in Fig. 5 and Fig. 6) are shown versus braking time in Fig. 7. It may be observed that unlike Fig. 5 and Fig. 6 the biggest temperature differences concentrate at about half of the braking time for both of the pad materials (Fig. 6a, b) and then decreases to equalize at the end of the process.

perature is slower dissipated through conduction giving bigger temperature gradients. Even at the end of the process the temperature is not equal within the disc thickness both with the pad made of FMK-845 and FMK-11. However the highest temperature obtain during the process $T = 461.4$ °C occurs for the friction pair made of steel EI-696/FMK-845 (Fig. 8a). The same relationship took place for the disc made of cast iron ChNMKh (Fig. 6).

Fig. 7. Evolutions of temperature at the pad/disc interface for different radial positions, solid curves indicate temperature-independent thermophysical properties whereas dashed curves thermosensitive materials:
a) disc (steel EI-696)/ pad (FMK-845)
b) disc (steel EI-696)/pad (FMK-11)
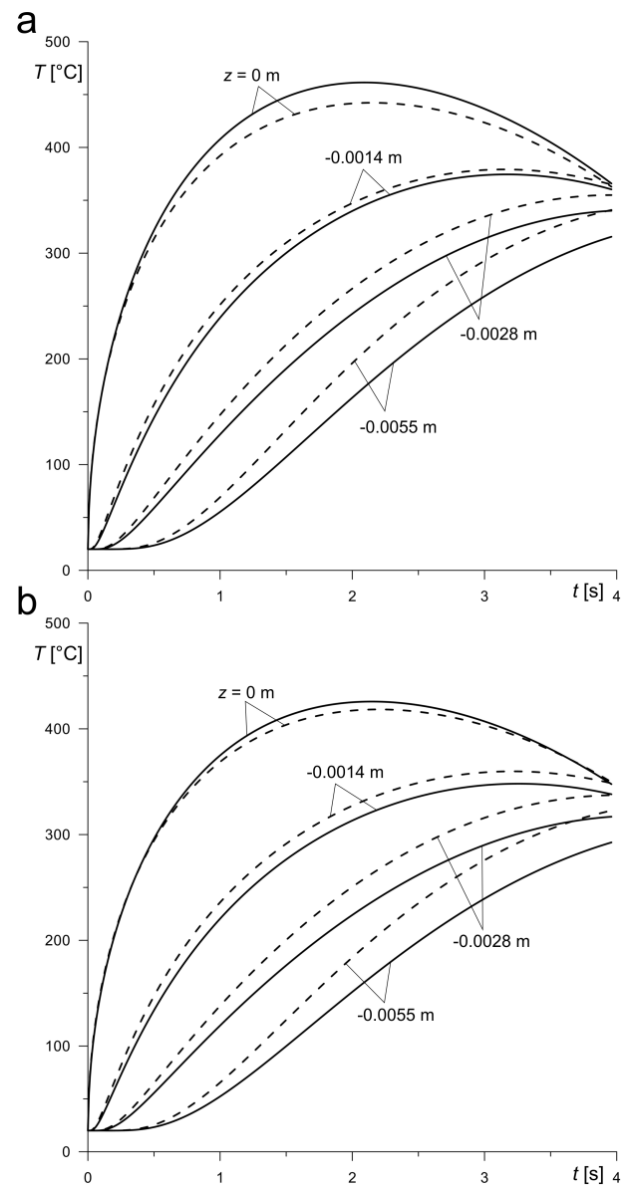
Fig. 8. Evolutions of temperature at selected axial positions of a disc (r = 0.095 m), solid curves indicate temperature-independent thermophysical properties, dashed curves thermosensitive materials: a) disc (steel EI-696)/pad (FMK-845) b) disc (steel EI-696)/pad (FMK-11)

Fig. 8 shows the temperature evolutions at specified axial locations (mean radius $r = 0,095$ mm) whose values correspond with Fig. 6. Spread of the subsequent temperatures at $z = 0$, -0,0014, -0,0028, -0,0055 m is clearly bigger than in Fig. 6 due to different material of the disc. In this case the disc made of steel EI-696 has the thermal conductivity about three times lower. Thereby the generated tem-

The temperature evolutions on the contact surface at three different distances from the axis of rotation during twofold braking process $t_s = 40$ s are shown in Fig. 9. The disc made of steel EI-696 was combined with the pad made of FMK-845 (Fig. 9a) and FMK-11 (Fig. 9b). According to the braking schema time from 0 to 3.96 s corresponds to the braking with constant deceleration to standstill followed by the disengagement of the brake components and simultane-

ous acceleration of the vehicle to the prior velocity of 100 km/h. Then the process was repeated which clearly affected the temperature evolutions. Unlike the single braking in the analyzed cases of twofold braking the temperature of the model with thermosensitive materials was lower in all cases. The occurred phase of vehicle acceleration reveals opposite situation either for FMK-845 or FMK-11. This relation loses its meaning during the second acceleration introducing some inconsistency. However for the friction pair steel EI-696/FMK-11 the rule that the temperature is higher for constant properties of materials was remained.
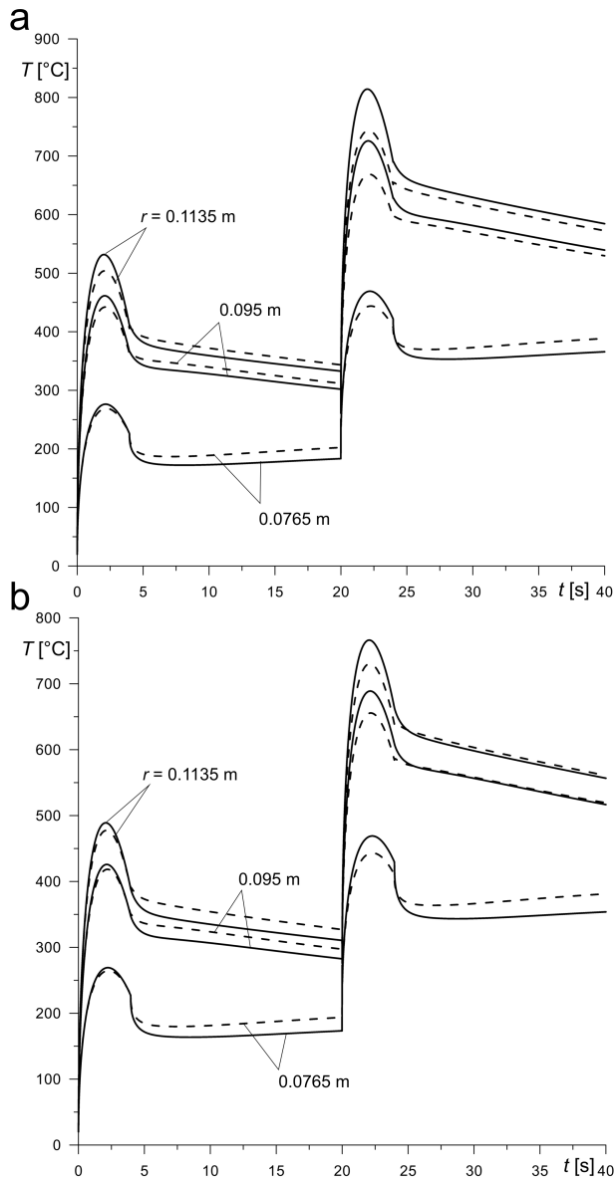
Fig. 9. Evolutions of temperature at the pad/disc interface during twofold braking process

Fig. 10 shows the temperature evolutions at selected axial positions z for the constant value of the radius $r = 0,095$ m. The process of the vehicle acceleration, just after the braking stage results in the temperature equalization (Fig. 10a, b) within the entire depth and its further linear decrease evoked by the cooling according to Newton's law. It may be observed that for both of friction pairs, the first

and the second brake application doesn't generate the same behaviour of temperature regarding the case with temperature-dependent and independent material properties. In the figure solely disc temperature are shown. The noticeable jump of temperature after the coupling of the disc and the pad at time $t = 20$ s stems from the temperature difference between these components after their disconnection and cooling conditions (Fig. 10 a, b).
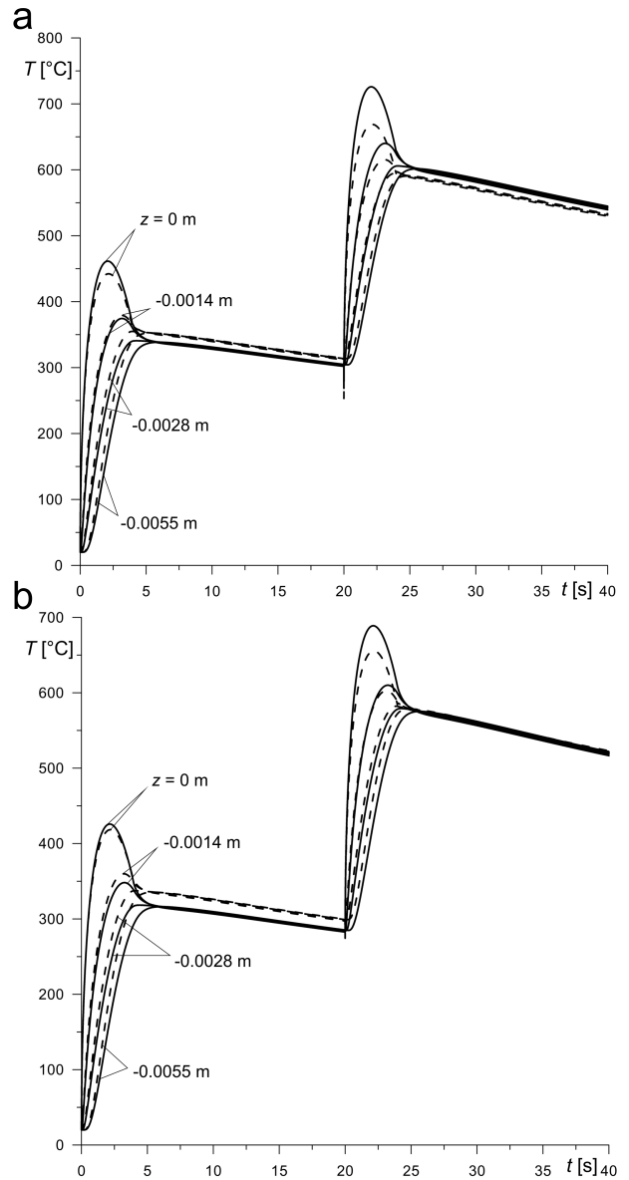
Fig. 10. Evolutions of temperature at different axial positions ($r = 0,095$ m) during twofold braking process

6. CONCLUSIONS

In this paper axisymmetric thermal analysis by using axisymmetric FE contact model was carried out to study an effect of the use of thermosensitive and temperature-independent thermophysical properties of materials on the temperatures of the pad/disc system during single and two-fold braking. The calculated temperatures on the friction surfaces as well as values at the selected axial locations

were confronted and compared. The obtained results reveal that within the range of temperatures variations from 20 to 800 °C of the brake components, in spite of relatively marked fluctuations of the thermophysical properties the use of subsequent constant values corresponding to 20 °C is validated. Both single and twofold braking confirms that rule. However relationship between the resulting temperature values obtained during computations by means of thermosensitive properties and temperature-independent constants varies during the twofold braking. It was observed that direct relation between the thermal effusivity and the resulting temperature is evident.

REFERENCES

1. **Adamowicz A., Grzes P.** (2011a), Analysis of disc brake temperature distribution during single braking under non-axisymmetric load, *Applied Thermal Engineering*, Vol. 31, No. 6-7, 1003-1012.
2. **Adamowicz A., Grzes P.** (2011b), Influence of convective cooling on a disc brake temperature distribution during repetitive braking, *Applied Thermal Engineering*, Vol. 31, No. 14-15, 2177-2185.
3. **Aderghal N., Loulou T., Bouchoucha A., Rogeon P.** (2011), Analytical and numerical calculation of surface temperature and thermal constriction resistance in transient dynamic strip contact, *Applied Thermal Engineering*, Vol. 31, No. 8-9, 1527-1535.
4. **Chichinadze A. V., Braun E. D., Ginsburg A. G., et al.** (1979), *Calculation, test and selection of frictional couples*, Nauka, Moscow, (in Russian).
5. **Ginzburg A. H.** (1973), Theoretical and experimental bases for calculation of unitary process of braking by means of system of the equations of thermal dynamics of friction, In: *Optimum use of frictional material in units of friction of machines*, Nauka, Moscow, 93-105, (in Russian).
6. **Grzes P.** (2009), Finite element analysis of disc temperature during braking process, *Acta Mechanica et Automatica*, Vol. 3, No. 4., 36-42.
7. **Grzes P.** (2009), Finite element analysis of disc temperature during braking process, *Acta Mechanica et Automatica*, Vol. 3, No. 4., 36-42.
8. **Grzes P.** (2010), Finite element analysis of temperature distribution in axisymmetric model of disc brake, *Acta Mechanica et Automatica*, Vol. 4, No. 4., 3-28.
9. **Grzes P.** (2011), Partition of heat in 2D finite element model of a disc brake, *Acta Mechanica et Automatica*, Vol. 5, No. 2, 35-41.
10. **Lee K., Barber J. R.** (1994), An Experimental Investigation of Frictionally-Excited Thermoelastic Instability in Automotive Disk Brakes Under a Drag Brake Application, *Journal of Tribology*, Vol. 116, No. 3, 409-414.
11. **Nosko A. L., Belyakov N. S., Nosko A. P.** (2009), Application of the generalized boundary condition to solving thermal friction problems, *Journal of Friction and Wear*, Vol. 30, No. 6, 455-462.
12. **Scieszka S. F.,** (1998) *Hamulce cierne – zagadnienia materiałowe, konstrukcyjne i tribologiczne*, ITE, Radom.
13. **Scieszka S., Zolnierz M.** (2007) The effect of the mine winder disc brake's design feature on its thermoelastic instability. Part I. Set-up for finite element modelling and numerical model verification, *Problems of Machines Operation and Maintenance* Vol. 42, No. 3, 111-124.
14. **Scieszka S., Zolnierz M.** (2007), The effect of the mine winder disc brake's design feature on its thermoelastic insta-

bility. Part II. Finite element simulation, *Problems of Machines Operation and Maintenance* Vol. 42, No. 4, 183-193.
15. **Sergienko V. P., Tseluev M. Yu., Kupreev A. V.** (2009), Numerical simulation of operation heat modes of multidisc oil-cooled vehicle brake. Part 1. Heat problem solution, *Journal of Friction and Wear*, Vol. 30, No. 5, 341-349.
16. **Talati F., Jalalifar S.** (2009), Analysis of heat conduction in a disk brake system, *Heat and Mass Transfer*, Vol. 45, No. 8, 1047-1059.
17. **Thuresson D.** (2004), Influence of material properties on sliding contact braking applications, *Wear*, Vol. 257, No. 5-6, 451-460.
18. **Wawrzonek L., Bialecki R.A**. (2008), Temperature in a disk brake, simulation and experimental verification, *International Journal of Numerical Methods for Heat & Fluid Flow*, Vol. 18, No. 3-4, 387-400.
19. **Yevtushenko A., Grzes P.** (2010), FEM-modeling of the frictional heating phenomenon in the pad/disc tribosystem (a review), *Numerical Heat Transfer Part A*, Vol. 58, No. 3, 207-226.
20. **Yevtushenko A., Grzes P.** (2011), Finite element analysis of heat partition in a pad/disc brake system, *Numerical Heat Transfer Part A*, Vol. 59, No. 7, 521-542.
21. **Yi Y.-B., Barber J. R., Hartsock D. L.** (2002), *Thermoelastic instabilities in automotive disc brakes-finite element analysis and experimental verification, in: J.A.C. Martins, D.P. Manuel, M. Marques (Eds.), Contact Mechanics*, Kluwer, Dordrecht, 187-202.
22. **Zhu Z.-C., Peng Y.-Z., Chen G.-A.** (2009), Three-dimensional transient temperature field of brake shoe during hoist's emergency braking, *Applied Thermal Engineering*, Vol. 29, No. 5-6, 932-937.